9th Biennial International Conference
& Exposition on Petroleum Geophysics

"HYDERABAD 2012"

P-246

Variable-depth streamer acquisition: broadband data for imaging and inversion

Robert Soubaras, Yves Lafet and Carl Notfors* , *CGGVeritas*

Summary

This paper revisits the problem of receiver deghosting, showing that for optimal signal-to-noise ratio it should be performed post-stack rather than pre-stack, as is the usual practise. A new deghosting algorithm is described, based on computing both a migration and a mirror migration and performing a joint deconvolution of the two. This method is true amplitude, as it is able to extract the true deghosted reflectivity, i.e. the reflectivity that would have been obtained had the water surface not been reflecting. The paper then describes how this new technique provides a method of deghosting data acquired with ghost notch diversity, such as slant streamer acquisition. We revisit this acquisition technique with two modifications. Firstly, we optimize the streamer-depth profile in order to ensure diversity for all reflector depths, resulting in a variable- depth streamer rather than a slant streamer. Secondly, since we recognize that stacking performs imperfect deghosting, leaving a residual ghost, we use our new deghosting technique to perform residual deghosting. This variable-depth streamer acquisition and processing has been employed in several locations. Here, we show results from West African, where a 2.5-150Hz bandwidth was achieved, and Western Australia. The broad bandwidth translates into improved results for acoustic impedance inversion. Variable-depth streamer data has the potential to fill the usual gap between the high frequencies of the seismic velocities and the low frequencies of the reflectivity, the 2.5-5 Hz octave being the overlap zone.

Keywords*: Broadband, Marine Acquisition, Inversion*

Introduction

Traditionally, receiver deghosting includes the zero-offset receiver ghost in the far-field signature and performs 1D deconvolution of the dataset at the preprocessing stage. The receiver ghost can be described as:

$$G(f) = 1 - e^{2j\pi 2\Delta z f/c} \quad (1)$$

where Δz is the depth of the streamer and c is the water velocity. This approach can be refined by taking the angle of propagation of the wavefield into account, instead of assuming vertical propagation, so that the ghost takes the form:

$$G(f, k_x, k_y) = 1 - e^{2j\pi 2\Delta z\sqrt{\frac{f^2}{c^2}-k_x^2-k_y^2}} \quad (2)$$

There are two problems raised by this approach. Firstly, although it is easy to account for non-vertical propagation in the inline direction x (parallel to the streamers), it is much more difficult to account for propagation in the crossline direction, y, due to the coarse sampling in this direction typically produced by multi-streamer acquisition. Secondly, as a general principle, any deconvolution of a redundant measurement with a variable wavelet should be performed after stack; therefore, since the deghosting operator is variable, it should be performed after stack rather than during preprocessing.

Optimal stacking with a variable wavelet

The optimal solution of the multichannel deconvolution problem:

$$T_n(f) = W_n(f)R(f) + E_n(f), n = 1, .., N \quad (3)$$

is not the pre-stack deconvolution plus stack formula:

$$\hat{R}(f) = \frac{1}{N}\sum_{n=1}^{N}\frac{T_n(f)}{W_n(f)} \quad (4)$$

but the least squares formula:

CGGVeritas, 9 Serangoon North Ave 5, Singapore 554531.
carl.notfors@cggveritas.com

$$\hat{R}(f) = \frac{\sum_{n=1}^{N} \overline{W_n(f)} T_n(f)}{\sum_{n=1}^{N} |W_n(f)|^2} \qquad (5)$$

which corresponds to matched filtering, stacking and post-stack deconvolution. Pre-stack deconvolution is only valid where the wavelets $W_n(f)$ do not depend on n. The more diversity there is in the wavelets, the more advantage there is in using the least squares formula.

Equation (5) is correct for a 1D wavelet. In order to account for all the angles of propagation (including crossline) that occur in multi-streamer acquisition, the multi-dimensional matched filtering can be realized by a "matched mirror migration". The matched mirror migration is defined as a migration in which the receivers are duplicated by introducing a mirror receiver at $(x_r,y_r,-z_r)$, recording the data $-d_r(t)$, for each actual receiver at (x_r,y_r,z_r), recording the data $d_r(t)$. The stacked matched mirror image is the equivalent of the numerator of equation (5). Spectral whitening by a zero-phase operator is a possible equivalent of division by the denominator but it is not true amplitude, as a white reflectivity assumption has to be made. For true amplitude deghosting we consider the two components of the matched mirror migration separately, the normal migration of the actual receivers, and the mirror migration of the mirror receivers. In the normal migration, the primary events are perfectly stacked, while the imperfectly stacked ghost events are present in the form of a causal residual ghost wavelet. Conversely, in the mirror migration, the ghost events are perfectly stacked with their polarity reversed, whilst the imperfectly stacked primary events are present in the form of an anti-causal residual wavelet. The proposed deghosting method uses this dual imaging of the same reflectivity with two different viewpoints to extract the true amplitude deghosted migration that would have been obtained by a conventional migration if the water-surface was non-reflective.

Joint Deconvolution

In conventional deconvolution (Robinson and Treitel, 1964), given a trace $d(t)$, we need to find a minimum phase wavelet $a_{min}(t)$ and a reflectivity $r(t)$ such that:

$$d(t) = a_{min}(t) * r(t) \qquad (6)$$

This problem is mathematically ill-posed, which is why we must assume the reflectivity $r(t)$ is white.

It is reasonable to assume that the ghost wavelet is a minimum phase signal, or at least a marginally minimum phase signal, and also that the mirror migration gives the same reflectivity as the migration, but distorted by a ghost wavelet that is maximum phase. The joint deconvolution problem then becomes one of given two signals, $d_1(t)$ and $d_2(t)$, to find a signal $r(t)$, a normalized minimum phase operator of given length $g_{min}(t)$ and a normalized maximum phase operator of given length $g_{max}(t)$ such that:

$$\begin{aligned} d_1(t) &= g_{min}(t) * r(t) \\ d_2(t) &= g_{max}(t) * r(t) \end{aligned} \qquad (7)$$

In an intuitive way, we can say that we have a binocular vision of the reflectivity, $r(t)$, with the conventional migration image, $d_1(t)$, coloured by a normalized minimum phase distortion, and the mirror migration image, $d_2(t)$, coloured by a normalized maximum phase distortion. Joint deconvolution recovers the reflectivity in true colour (i.e. without distortion). Although the joint deconvolution, equation (7), looks very similar to conventional deconvolution, equation (6), this is a well-posed problem, which means it has a unique solution, even when the minimum phase and maximum phase properties are marginally respected (i.e. the operators have perfect spectral notches) (Soubaras, 2010). No assumption is needed regarding the amplitude spectrum of the reflectivity, which is arbitrary and unknown. It can be proved mathematically that, since a minimum phase signal is causal and has a causal inverse and a maximum phase signal is anti-causal and has an anti-causal inverse, this joint deconvolution has a unique solution (Soubaras 2011). The joint deconvolution can be performed in a least squares sense where there is noise in the data, and can also be performed in a multichannel manner.

Variable-depth streamer acquisition

Although this deghosting method can be used with any kind of acquisition geometry, it is particularly suited to variable-depth acquisitions exhibiting pre-stack notch diversity. This pre-stack notch diversity prevents perfect notches being present on the post-stack data. After migration and mirror migration, the residual ghosts have no perfect notches (apart from frequency zero), and so can be estimated and deconvolved using the joint deconvolution method. Since the deghosted image uses both the migration

and the mirror migration, it benefits from"fold doubling", using both primary and ghost events to build the image. In slant streamer acquisition, where the streamer depth increases linearly with offset, current streamer lengths cannot provide sufficient notch diversity for shallow events, which do not use the whole length of the streamer. Therefore it is necessary to optimize the streamer depth profile in order to ensure diversity for all reflector depths. This profile can be tuned to provide the maximum possible bandwidth for a given geological setting and water depth.

This technique takes full advantage of towing solid streamers at what are currently considered as extreme depths, in order to benefit from the improved low-frequency response of the hydrophones and reduced sea-state noise. To date a variety of surveys have been acquired in different settings with maximum streamer depths as large as 60m. The flexibility means that the method can be used for a range of applications. The increase in penetration from the extension of the bandwidth at the low end benefits the imaging of deep targets and those below complex overburdens. Shallow targets (such as shallow hazards) benefit from the total bandwidth available and recordable. Usable bandwidths between 2.5 and 160 Hz have been recorded.

Some data was acquired offshore West Africa using the variable-depth streamer technique. The processing flow applied to this consisted of source designature, surface-related multiple elimination, time-migration (normal and mirror) and joint deconvolution. No spectral shaping was performed, so the section can be considered as being not only true amplitude but also true spectrum. The result is shown in Figure 2, and has a bandwidth of 2.5-150 Hz as seen in Figure 4-a. The broadband nature of this image, in terms of both low and high frequencies, together with its low-noise character, can be compared with the conventional image shown in Figure 1. This was obtained by processing data from conventional acquisition performed along the same 2-D line and recorded with the same equipment, just prior to the variable-depth streamer line. These data were processed using a similar flow, apart from the receiver deghosting which was performed in the conventional manner, by including the receiver ghost in the source designature, instead of by joint deconvolution.

Example inversion results from West Africa

Variable-depth streamer data provide significant benefits for seismic inversion workflows, especially in terms of low frequency bandwidth extension. The lack of low frequencies in conventional seismic data means that a low frequency model must be incorporated in the inversion process in order to recover absolute impedance values. Usually, the low-frequency information is obtained by interpolating low-passed filtered impedance logs between well locations, using interpreted horizons as a guide. If the wells are sparse and the geology complex, the low frequency model derived from the wells may be inaccurate and yield biased inversion results. The typical solution is to use NMO-derived seismic velocities to define the background low frequency model. However, while the seismic velocities provide information at very low frequencies (~0-4 Hz), they are not usually suitable to infill the missing frequencies in the range of 4-10 Hz.

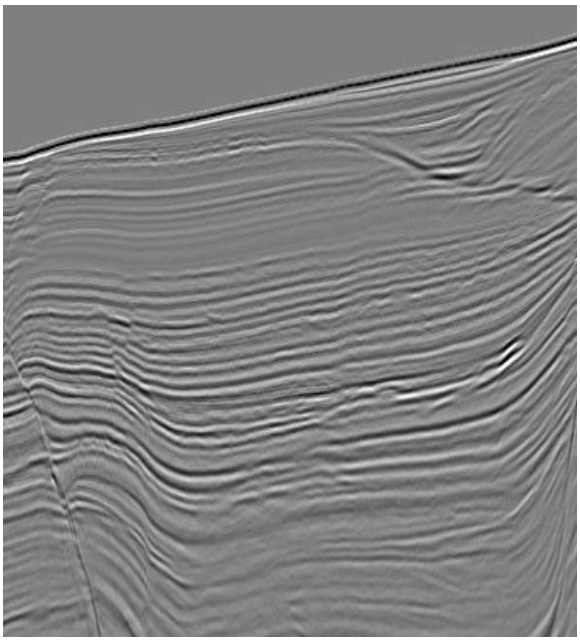

Figure 1. Conventional image

With variable-depth streamer data, these missing frequencies can be recovered, reducing the need to build a low frequency inversion model from well data. The interval velocities derived from the high resolution V_{rms} field obtained during the processing of the variable-depth streamer data are shown in red in Figure 3. A very good

match can be seen with the well velocities, shown in black, although the well information was not used to derive the red curve, which was derived solely from the V_{rms} field.

In order to quantify the benefits of the improved low frequency content on seismic inversion, we have performed comparative acoustic impedance (Ip) inversion tests using both the conventional and the variable-depth streamer data from West Africa. Figure 4-a shows a comparison of the power spectra of the two datasets. The low frequency (0-5Hz) initial model was constructed from the seismic velocities of the variable-depth streamer data (Figure 4-b) and used to constrain both inversions. Log data from a well located near the seismic line were used only to validate the wavelets and seismic velocities, and to QC the inversion results. Figures 4-c and 4-d respectively show the absolute acoustic impedance profile estimated from the conventional and variable-depth streamer data. The two arrows displayed on the variable-depth streamer inversion results indicate the position of two thick sediment wedges whose shape is much better delineated than in the inversion of the conventional data.

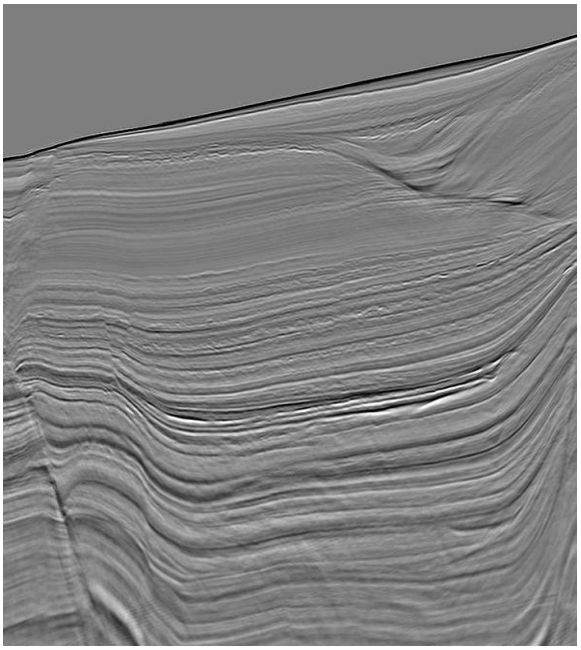

Figure 2. Variable depth streamer image

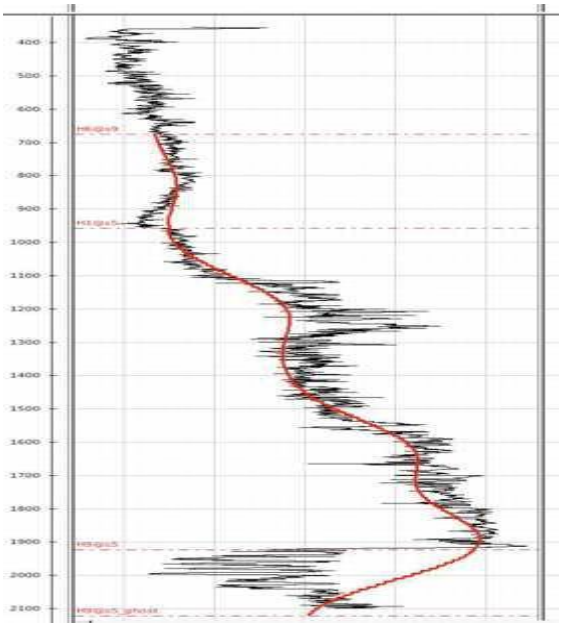

Figure 3. Black: velocity from well data. Red: interval velocity computed from the Vrms velocities of the variable-depth streamer data

The impact of the additional low frequencies can be evaluated directly by subtracting the initial model from the inversion results, as shown in Figure 4-e and 4-f. The thick bands (~100msec) of negative and positive relative impedances, that are visible on the right hand side of Figure 4-f, result directly from the extension of the low frequency bandwidth achieved with the variable-depth streamer data. In view of the structural complexity, as well as the absence of well data on the right hand side of the line, it would have been difficult to use standard well log extrapolation to recover the missing low frequency component in the inversion of the conventional data. The high frequency content of the variable-depth streamer data (Figure 4-a) is also expected to significantly enhance inversion quality for detailed reservoir characterization work. In the exploration example illustrated above, we chose to limit the high frequency content of the inversion by working in a relatively coarse (8 msec) layered framework adapted to the vertical resolution of conventional data processing.

Additional inversion results from Western Australia

A further data comparison was acquired offshore Western Australia. For this comparison one well was excluded from the initial model-building and compared with the results from the inversion of both conventional and variable-depth

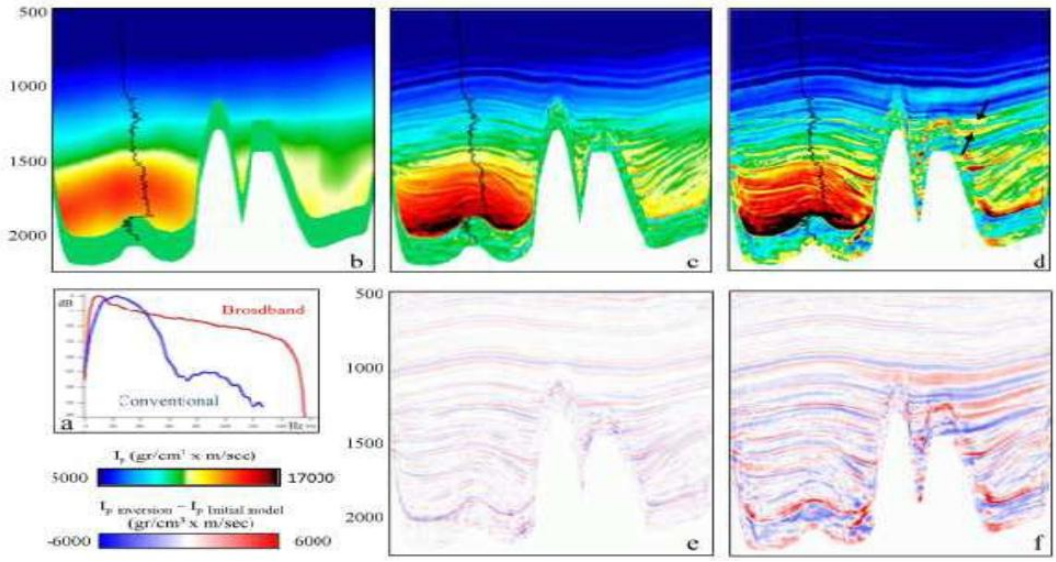

Fig. 4: Acoustic inversion results. a) Spectra of conventional and variable-depth streamer data. b) Initial model. c) Conventional data inversion. d) Variable-depth streamer data inversion.

streamer data. The low frequencies provided by the variable-depth streamer data provided a much better prediction of the shape of the acoustic impedance at the blind well than that obtained from the conventional data (see Figures 5 and 6). This proves that the low frequencies being achieved are providing real information that translates into real improvements in the inversion results.

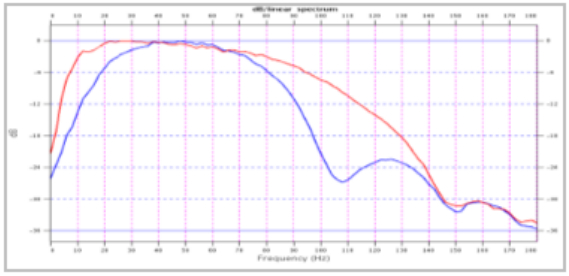

Figure 6. Normalised spectrum from 1.8 – 3.5s. Blue line = conventional data, red line= variable depth streamer data e) ΔIp between conventional inversion and initial model f) ΔIp between variable-depth streamer data inversion and initial model

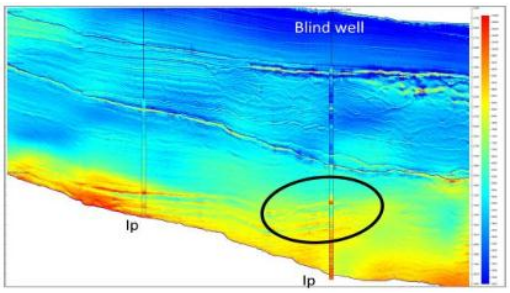

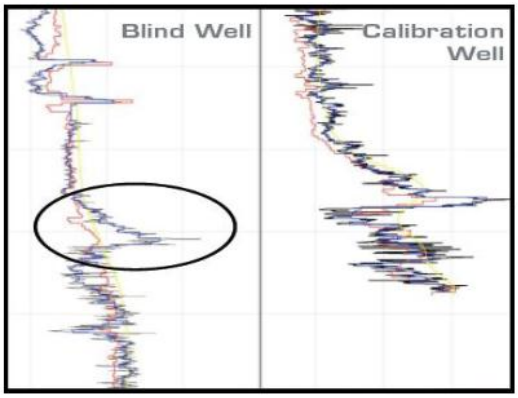

Figure 7(a) Acoustic impedance from inversion of conventional data

Conclusion

We have described a new deghosting method that is performed at the imaging stage of the processing sequence rather than the preprocessing stage, in order to ensure the best signal-to-noise ratio. The method jointly deconvolves the migration and the mirror migration of the data. This deghosting method is true amplitude, retrieving the migration of the unghosted modeled data from the ghosted modeled data. This deghosting method is ideal for the processing of variable-depth streamer acquisitions. With such an acquisition and processing method, we have achieved a bandwidth of six octaves (2.5 – 160Hz) on real data. Inversion results have been shown to benefit from this enhanced bandwidth. In particular, variable-depth streamer data seems to have the potential to fill the usual gap between the high frequencies of the seismic velocities and the low frequencies of the reflectivity, tp produe more reliable well predictions.

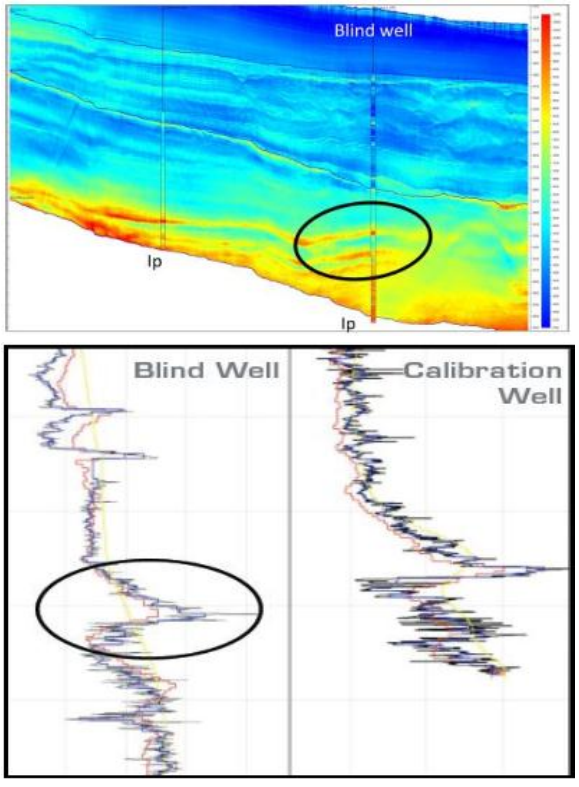

Figure 7(b) Acoustic impedance from inversion of variable-depth streamer data.

References

Robinson, E. A., and S. Treitel, 1964, Principles of digital filtering: Geophysics, **61**, 345–404.

Soubaras, R., 2010, Deghosting by joint deconvolution of a migration and a mirror migration: 80th Annual International Meeting, SEG, Expanded Abstracts, 3406–3409.

Acknowledgements

We thank Total, the Republic of Gabon and Cobalt for permission to show the real data examples from West Africa.

We thank CGGVeritas for permission to publish this work and to show the Western Australia data examples.